

Magnetic fluctuations and superconductivity in iron pnictides as probed by electron spin resonance

N. Pascher,¹ J. Deisenhofer,^{1,*} H.-A. Krug von Nidda,¹ M. Hemmida,¹ H. S. Jeevan,² P. Gegenwart,² and A. Loidl¹

¹*Experimentalphysik V, Center for Electronic Correlations and Magnetism, Institute for Physics, Augsburg University, D-86135 Augsburg, Germany*

²*I. Physik. Institut, Georg-August-Universität Göttingen, D-37077 Göttingen, Germany*

(Received 22 December 2009; revised manuscript received 10 June 2010; published 30 August 2010)

The electron spin resonance (ESR) absorption spectrum of Eu^{2+} ions serves as a probe of the normal and superconducting state in $\text{Eu}_{0.5}\text{K}_{0.5}\text{Fe}_2\text{As}_2$. The spin-lattice relaxation rate $1/T_1^{\text{ESR}}$ obtained from the ESR linewidth exhibits a Korringa-type linear increase with increasing temperature above T_c evidencing a normal Fermi-liquid behavior. Below 45 K deviations from the Korringa law occur which are ascribed to enhanced magnetic fluctuations within the FeAs layers upon approaching the superconducting transition. Below T_c the spin lattice relaxation rate $1/T_1^{\text{ESR}}$ follows a $T^{1.5}$ behavior without any appearance of a coherence peak.

DOI: [10.1103/PhysRevB.82.054525](https://doi.org/10.1103/PhysRevB.82.054525)

PACS number(s): 76.30.-v, 74.70.Xa

I. INTRODUCTION

The recent discovery of superconductivity in Fe-based pnictides and chalcogenides¹⁻⁴ has triggered enormous research efforts to understand the origin of superconductivity and its relation to the inherent magnetism of iron. One class of these materials are the ternary $A\text{Fe}_2\text{As}_2$ systems with $A = \text{Ba}, \text{Sr}, \text{Ca}, \text{Eu}$ (122-systems) and T_c values up to 38 K.^{3,5-7} The parent compounds exhibit a spin-density wave (SDW) anomaly accompanied by a structural distortion.^{8,9} Superconductivity (SC) appears, e.g., by substituting the A-site ions by K (Refs. 3 and 5) or Fe by Co.^{6,7} For underdoped $\text{Ba}_{1-x}\text{K}_x\text{Fe}_2\text{As}_2$ and Co-doped BaFe_2As_2 a coexistence of the SDW state and superconductivity has been reported.⁹⁻¹⁴

A particularly interesting 122-system is EuFe_2As_2 with $T_{\text{SDW}} = 190$ K,¹⁵⁻¹⁷ the highest reported SDW transition temperature in the pnictides. This system is of special importance among the 122 iron pnictides since the antiferromagnetic ordering of local Eu^{2+} moments at $T_N = 19$ K provides the opportunity to study the interplay between Eu and Fe magnetism and also the influence of Eu magnetism on SC (under hydrostatic pressure¹⁸ or doping^{5,19,20}). The appearance of a SDW gap in EuFe_2As_2 was evidenced by optical spectroscopy¹⁷ and, recently, the opening of even two gaps with different characteristics was reported.²¹ Moreover, electron spin resonance (ESR) in single-crystalline EuFe_2As_2 revealed a drastic change in the magnetic properties of the Eu-spin system from a typical metalliclike behavior above T_{SDW} to a behavior characteristic for a magnetic and insulating system in the SDW state.²²

Here, we focus on $\text{Eu}_{0.5}\text{K}_{0.5}\text{Fe}_2\text{As}_2$ in which the iron SDW is completely suppressed by hole doping and SC is found below $T_c = 32$ K.⁵ The bulk nature of SC is confirmed by a clear specific-heat anomaly and diamagnetism found in dc-magnetization and ac-susceptibility measurements. After subtraction of the phonon contribution, a specific-heat jump height of about 70 mJ/mol K^2 has been deduced.²³ Mössbauer spectroscopy measurements have established the coexistence of Eu^{2+} short-range magnetic ordering with SC in $\text{Eu}_{0.5}\text{K}_{0.5}\text{Fe}_2\text{As}_2$ below 4.5 K.²⁴ At the same temperature, a peak is found in the zero-field cooled magnetization, mea-

sured at low fields of 5 mT,⁵ and a corresponding minimum occurs in the magnetic penetration depth $\lambda(T)$, determined by radio-frequency technique.²⁵ Recently, the substitution of Fe by Co in EuFe_2As_2 reportedly leads to an incomplete superconducting transition in the electrical resistivity.²⁰ SC has also been found in chemically pressurized $\text{EuFe}_2(\text{As}_{0.7}\text{P}_{0.3})_2$ at $T_c = 26$ K, followed by ferromagnetic Eu ordering at 20 K.¹⁹

In this work we show that the ESR signal of Eu^{2+} can be used as probe of the superconducting properties in the 122-family of Fe pnictides. In a metallic system the linewidth of the ESR absorption is a direct measure of the spin-lattice relaxation rate $1/T_1^{\text{ESR}}$, thus providing information on the density of states at the Fermi energy and the opening of the SC gap. In polycrystalline $\text{Eu}_{0.5}\text{K}_{0.5}\text{Fe}_2\text{As}_2$ we observe a clear change of $1/T_1^{\text{ESR}}$ from a normal Fermi-liquidlike behavior with a Korringa relaxation $\propto T$ above 45 K, the onset of magnetic fluctuations of the FeAs layers for $T_c < T < 45$ K, and a $\propto T^{1.5}$ law below $T_c = 32$ K.

II. EXPERIMENTAL DETAILS

Polycrystalline $\text{Eu}_{0.5}\text{K}_{0.5}\text{Fe}_2\text{As}_2$ was prepared using a sintering method described in Ref. 5 and characterized by energy-dispersive x-ray (EDX) analysis, x-ray, electrical resistivity, magnetic susceptibility, and specific-heat experiments.²³ ESR measurements were performed in a Bruker ELEXSYS E500 CW spectrometer at X-band frequencies ($\nu \approx 9.36$ GHz) equipped with a continuous He gas-flow cryostat in the temperature region $4.2 < T < 300$ K. ESR detects the power P absorbed by the sample from the transverse magnetic microwave field as a function of the static magnetic field H . The signal-to-noise ratio of the spectra is improved by recording the derivative dP/dH using lock-in technique with field modulation. The sample was measured in the form of fine powder.

III. EXPERIMENTAL RESULTS AND DISCUSSION

Figure 1 shows ESR spectra of a powdered polycrystal of $\text{Eu}_{0.5}\text{K}_{0.5}\text{Fe}_2\text{As}_2$ for different temperatures. In all cases one

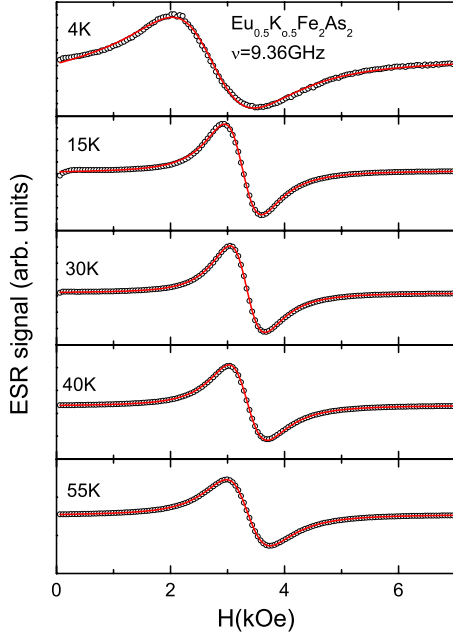


FIG. 1. (Color online) ESR spectra and corresponding fit curves of $\text{Eu}_{0.5}\text{K}_{0.5}\text{Fe}_2\text{As}_2$ at different temperatures below and above T_c .

observes a single exchange-narrowed resonance line which is well described by a Dyson shape,²⁶ i.e., a Lorentz line at resonance field H_{res} with half-width at half maximum ΔH and a contribution of the dispersion to absorption (D/A) ratio $0 \leq D/A \leq 1$, resulting in an asymmetry typical for metals where the skin effect drives electric and magnetic components of the microwave field out of phase. The D/A ratio is determined as a fit parameter and depends on sample size, geometry, and skin depth. If the skin depth is small compared to the sample size, D/A approaches 1. Focusing on the low-field regime, below the superconducting transition temperature T_c the spectra as documented in Fig. 2 exhibit a diplike signal at low fields typical for the magnetic shielding below the lower critical field $H_{c1} \approx 100$ Oe,²⁵ followed by a broad nonresonant microwave absorption feature due to the penetration of magnetic flux in the Shubnikov phase above H_{c1} of the type-II superconductor.²⁷

Returning to the resonant absorption we determined the absolute value of the ESR spin susceptibility χ_{ESR} above T_c

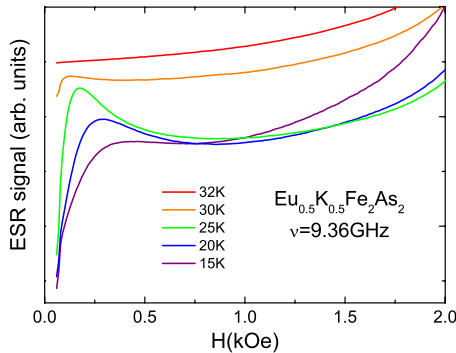


FIG. 2. (Color online) Temperature evolution of the low-field absorption spectra of $\text{Eu}_{0.5}\text{K}_{0.5}\text{Fe}_2\text{As}_2$ below T_c . Lines are shifted for clarity.

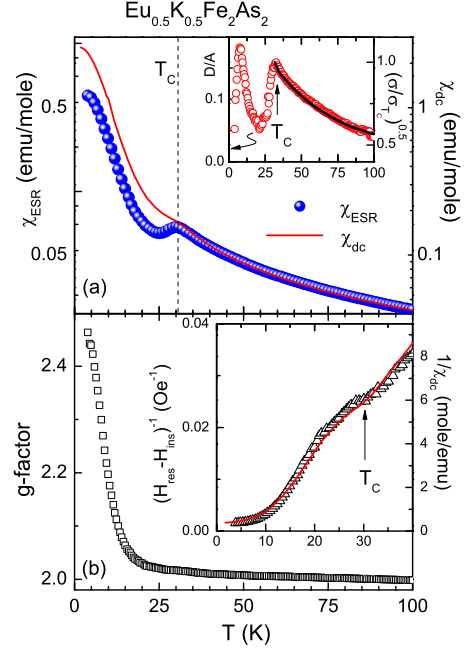


FIG. 3. (Color online) (a) Temperature dependence of the ESR intensity compared to the magnetic dc susceptibility (solid line) measured in a magnetic field of 0.3 T, i.e., well above the lower critical field H_{c1} in $\text{Eu}_{0.5}\text{K}_{0.5}\text{Fe}_2\text{As}_2$. Inset: temperature dependence of the dispersion to absorption ratio D/A compared to the square root of the normalized dc conductivity (solid line). (b) Temperature dependence of the g factor of the ESR line. Inset: inverse shift of the resonance field H_{res} from its insulator value H_{ins} given by $g_{\text{ins}} = 1.993$ compared to the inverse static susceptibility.

by comparison of the double-integrated signal intensity with that of the reference compound $\text{Gd}_2\text{BaCuO}_5$ —the so-called green phase—which exhibits an ESR signal with a similar linewidth. In $\text{Gd}_2\text{BaCuO}_5$ all Gd^{3+} spins (with the same electron configuration $4f^7$ and spin $S=7/2$ such as Eu^{2+}) contribute to the ESR signal and the corresponding susceptibility exhibits a Curie-Weiss law with $\Theta_{\text{CW}} = -23$ K.²⁸ We find that about 50% of the Eu^{2+} ions participate in the resonant absorption. Estimating the skin depth $\delta = (\rho / \mu_0 \omega)^{0.5}$ using the resistivity value $\rho = 0.04$ Ωcm at room temperature²⁴ and the microwave frequency 9 GHz we find a skin depth of $\delta \approx 75$ μm . The typical grain size of powdered samples is of the same order of magnitude in agreement with the percentage of Eu^{2+} spins contributing to the observed signal.

The temperature dependence of the double-integrated signal intensity χ_{ESR} is compared to the static susceptibility χ_{dc} in Fig. 3(a). Note the different scales due to the fact that only 50% of the Eu spins contribute to the resonant absorption. Starting from high temperatures the Curie-Weiss behavior of χ_{ESR} is interrupted just below T_c , where it abruptly decreases and again increases on further lowering the temperature, while the static susceptibility increases monotonously without any drop but only slightly deviating from the Curie-Weiss law at T_c . The temperature dependence of the D/A ratio is shown in the inset of Fig. 3(a) together with the square root of the normalized conductivity $[\sigma / \sigma(T=T_c)]^{0.5}$ in the normal state taken from Ref. 5. In the normal state the two quantities can be scaled to fall on top of each other,

confirming that D/A is proportional to the penetration depth of the microwave. The D/A ratio drops by a factor of 3 when crossing T_c with decreasing temperature. After the anticipated onset of enhanced magnetic fluctuations of the Eu ions at about 25 K it starts to increase again up to 8 K, below which D/A decreases again. The drop of intensity on passing T_c can be understood due to the fact that magnetic resonance is observed only from the volume fraction of the sample which is penetrated by the magnetic flux, i.e., the surface within the London penetration depth and—in superconductors of type II—the magnetic flux tubes with normal conductivity. The concomitant drop of the D/A ratio is difficult to explain because the superconductivity strongly reduces the skin depth and, hence, is naively expected to increase the D/A ratio. The observed decrease may presumably result from the change of the effective geometry of the normal-state regions, i.e., the flux tubes in the superconducting matrix instead of a homogeneously conducting state because the conductivity of these regions can be anticipated to be unchanged. Thus, the ratio of the skin depth to the diameter of the flux tubes is larger than the ratio of the skin depth to the full sample diameter, which can result in a decrease in the D/A ratio. However, detailed electro-dynamical considerations are necessary to clarify this observation. The consecutive increase of the D/A ratio on decreasing temperature can be related to the reentrant Eu magnetism which leads to an increase in the normally conducting volume fraction. Finally, the peak at about 8 K marks the onset of short-range order.^{24,25}

The temperature dependence of the g value depicted in the lower frame of Fig. 3 is only slightly affected by the onset of superconductivity. The g value is about 2 above T_c and starts to increase strongly below 25 K. The inset compares the corresponding inverse shift of the resonance field from its value in an insulating environment determined by $g_{\text{ins}}=1.993$ (see Ref. 29) to the inverse static susceptibility. Both quantities approximately coincide showing that the resonance shift is dominated by demagnetization fields resulting from the large Eu magnetization similar to observations in systems such as GdI_2 or YBaMn_2O_6 .^{30,31} Only the small kink at T_c in both the reciprocal susceptibility and the resonance shift can be regarded as an effect of the superconducting state due to the opening of the excitation gap in the electronic density of states at the Fermi level and corresponding reduction in the Pauli contribution to the susceptibility. The g shift at elevated temperature $\Delta g = g - g_{\text{ins}} = J_{\text{CE-Eu}}(0)N(E_F) \approx 0.02$ results from the homogenous polarization of the conduction electrons in the external field (Pauli susceptibility) and is comparable to usual metals.³²

Now we will turn to the temperature dependence of the ESR linewidth shown in Fig. 4. Note that in metallic systems the ESR linewidth is determined by the spin-lattice relaxation time T_1 (Ref. 26) and, hence, provides information complementary to NMR or nuclear quadrupole resonance (NQR) measurements. One can clearly identify a linear increase with temperature with a slope $b=5.1$ Oe/K and a residual zero-temperature width $\Delta H_0=374$ Oe. Upon entering the superconducting state, a pronounced drop of the linewidth can be recognized in the inset of Fig. 4. Below about 20 K the linewidth increases again due to growing magnetic

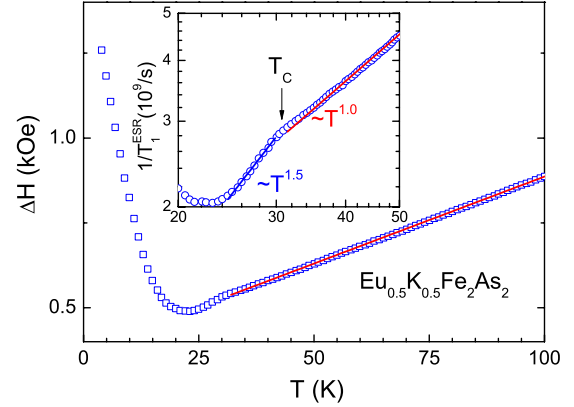


FIG. 4. (Color online) Temperature dependence of the ESR linewidth ΔH . The solid line indicates the linear Korringa law. Inset: temperature dependence of $1/T_1^{\text{ESR}}$ on a double-logarithmic scale and linear fits indicating the power laws in the normal and SC states.

fluctuations of the Eu spins on approaching short-range order.

The observed linear increase in the linewidth $\Delta H \propto \langle J_{\text{CE-Eu}}^2(q) \rangle N^2(E_F)T$ (Korringa relaxation) is a typical signature of local moments in a Fermi liquid and depends on the conduction-electron density of states $N(E_F)$ at the Fermi energy E_F and the exchange coupling $J_{\text{CE-Eu}}$ between the conduction electrons and the Eu spins. The observed slope of 5.1 Oe/K is a usual value for S state $4f^7$ local moments in metals and indicates a normal three-dimensional Fermi-liquid state.^{26,32,33} In case of ferromagnetic correlations between the Eu ions (reading off the Curie-Weiss temperature from the inset in the lower panel of Fig. 3 gives $\Theta_{\text{CW}} \approx 10$ K) the residual linewidth is expected to be negative $\Delta H_0 = -b\Theta_{\text{CW}} \approx -50$ Oe with b being the derived Korringa slope.²⁶ The larger positive value $\Delta H_0=374$ Oe is probably due to an inhomogeneous distribution of the Eu and K ions, a problem which is well known for the 122-systems. This may lead to strong fluctuations of the long-range dipolar fields while the narrowing effect of the short-range exchange narrowing is reduced.

In the inset of Fig. 4 we show the temperature dependence of the reciprocal electron spin-lattice relaxation time given by

$$1/T_1^{\text{ESR}} = \gamma(\Delta H - \Delta H_0), \quad (1)$$

where $\Delta H_0=374$ Oe is the residual zero-temperature linewidth obtained from the linear fit in the normal regime and γ denotes the gyromagnetic ratio. The obtained power law in the normal state clearly confirms the Korringa law, but for the superconducting state we observe a behavior $\propto T^{1.5}$ without any indication of a coherence (Hebel-Slichter) peak, ruling out a conventional BCS scenario with an isotropic gap. Due to the onset of magnetic fluctuations the ESR power law can only be traced in a narrow temperature range below T_c and we cannot exclude the possibility that $1/T_1^{\text{ESR}}$ may be influenced by the vicinity of the short-range Eu interactions. To examine closer the vicinity of T_c we plot $1/(T_1^{\text{ESR}}T)$ as a function of temperature in Fig. 5. A clear increase from the

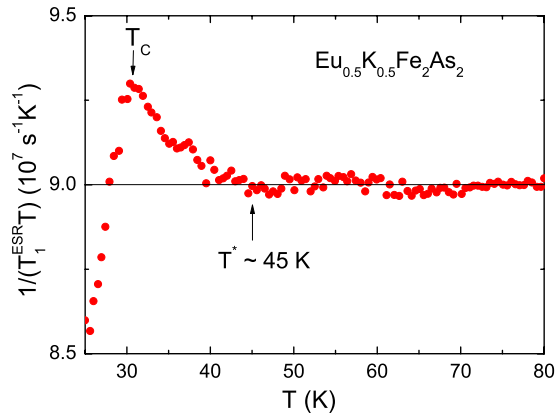


FIG. 5. (Color online) Temperature dependence of $1/(T_1^{\text{ESR}}T)$. The solid line indicates the linear Korringa law. Below $T^* \approx 45$ K a deviation from the linear behavior indicates the onset of magnetic fluctuations on approaching the superconducting transition.

constant high-temperature (Korringa) value occurs already below a temperature $T^* \approx 45$ K and leads to a maximum and a sharp drop just below T_c . A similar behavior of the spin-lattice relaxation time of ^{57}Fe and ^{75}As above T_c has been reported by NMR in the related system $\text{Ba}_{0.6}\text{K}_{0.4}\text{Fe}_2\text{As}_2$ and attributed to spin fluctuations in the FeAs layers due to interband nesting.³⁴

A Korringa behavior in the normal state has also been found by ESR in pure and Co-doped EuFe_2As_2 (Refs. 22 and 35) and by NMR and NQR studies on other 122-compounds^{34,36} but in the superconducting state of Fe-based superconductors the temperature behavior of the nuclear spin-lattice relaxation time has revealed nonuniversal power laws $1/T_1 \propto T^\alpha$ with α ranging from 2.5–6.^{34,36–38} We want to point out that an NQR study of pure KFe_2As_2 revealed a power law $\propto T^{1.4}$ similar to our ESR results which

was interpreted in terms of multigap superconductivity with line nodes³⁶ and a recent NMR study suggested that this exponent may be universal for overdoped $\text{Ba}_{1-x}\text{K}_x\text{Fe}_2\text{As}_2$.³⁹

Given the narrow temperature range of the ESR power law, we refrain at the present stage from performing a fit of the data, as the above-mentioned NMR studies showed that very different power laws can be obtained by varying the gaps' sizes and symmetry. However, our data nicely show that local-moment ESR in iron pnictides is a highly efficient tool to shed light on the superconducting order parameters as a complementary method to nuclear spin resonance techniques.

IV. SUMMARY

In summary, we show that the ESR signal of Eu^{2+} spins gives direct access to the superconducting state of the 122-class of pnictides. We identify a normal Fermi-liquid behavior above T_c from the Korringa law of the ESR spin-lattice relaxation rate $1/T_1^{\text{ESR}}$. Just above T_c we observe a deviation from the Korringa behavior which we assign to magnetic fluctuations in the FeAs layers on approaching the superconducting state. Below T_c no Hebel-Slichter peak is observed, ruling out a simple isotropic BCS scenario, and the spin-lattice relaxation rate follows $1/T_1^{\text{ESR}} \propto T^{1.5}$.

ACKNOWLEDGMENTS

We thank S. Graser for fruitful discussions, and A. Pimenova and V. Tsurkan for experimental support. We acknowledge partial support by the Deutsche Forschungsgemeinschaft (DFG) under the Schwerpunktprogramm Grant No. SPP1458, the Collaborative Research Center TRR 80, and the Research Unit FOR 960 (Quantum phase transitions).

*joachim.deisenhofer@physik.uni-augsburg.de

- ¹Y. Kamihara, T. Watanabe, M. Hirano, and H. Hosono, *J. Am. Chem. Soc.* **130**, 3296 (2008).
- ²X. H. Chen, T. Wu, G. Wu, R. H. Liu, H. Chen, and D. F. Fang, *Nature (London)* **453**, 761 (2008).
- ³M. Rotter, M. Tegel, and D. Johrendt, *Phys. Rev. Lett.* **101**, 107006 (2008).
- ⁴F.-C. Hsu, J.-Y. Luo, K.-W. Yeh, T.-K. Chen, T.-W. Huang, P. M. Wu, Y.-C. Lee, Y.-L. Huang, Y.-Y. Chu, D.-C. Yan, and M.-K. Wu, *Proc. Natl. Acad. Sci. U.S.A.* **105**, 14263 (2008).
- ⁵H. S. Jeevan, Z. Hossain, D. Kasinathan, H. Rosner, C. Geibel, and P. Gegenwart, *Phys. Rev. B* **78**, 092406 (2008).
- ⁶A. S. Sefat, R. Jin, M. A. McGuire, B. C. Sales, D. J. Singh, and D. Mandrus, *Phys. Rev. Lett.* **101**, 117004 (2008).
- ⁷A. Leithe-Jasper, W. Schnelle, C. Geibel, and H. Rosner, *Phys. Rev. Lett.* **101**, 207004 (2008).
- ⁸M. Rotter, M. Tegel, D. Johrendt, I. Schellenberg, W. Hermes, and R. Pöttgen, *Phys. Rev. B* **78**, 020503 (2008).
- ⁹M. Rotter, M. Tegel, I. Schellenberg, F. M. Schappacher, R. Pöttgen, J. Deisenhofer, A. Günther, F. Schrettle, A. Loidl, and D.

Johrendt, *New J. Phys.* **11**, 025014 (2009).

- ¹⁰M. Rotter, M. Pangerl, M. Tegel, and D. Johrendt, *Angew. Chem., Int. Ed.* **47**, 7949 (2008).
- ¹¹H. Chen, Y. Ren, Y. Qiu, Wei Bao, R. H. Liu, G. Wu, T. Wu, Y. L. Xie, X. F. Wang, Q. Huang, and X. H. Chen, *EPL* **85**, 17006 (2009).
- ¹²D. K. Pratt, W. Tian, A. Kreyssig, J. L. Zarestky, S. Nandi, N. Ni, S. L. Bud'ko, P. C. Canfield, A. I. Goldman, and R. J. McQueeney, *Phys. Rev. Lett.* **103**, 087001 (2009).
- ¹³A. D. Christianson, M. D. Lumsden, S. E. Nagler, G. J. MacDougall, M. A. McGuire, A. S. Sefat, R. Jin, B. C. Sales, and D. Mandrus, *Phys. Rev. Lett.* **103**, 087002 (2009).
- ¹⁴Ch. Kant, J. Deisenhofer, A. Günther, F. Schrettle, A. Loidl, M. Rotter, and D. Johrendt, *Phys. Rev. B* **81**, 014529 (2010).
- ¹⁵H. Raffius, M. Morsen, B. D. Mosel, W. Müller-Warmuth, W. Jeitschko, L. Terbüchte, and T. Vomhof, *J. Phys. Chem. Solids* **54**, 135 (1993).
- ¹⁶H. S. Jeevan, Z. Hossain, D. Kasinathan, H. Rosner, C. Geibel, and P. Gegenwart, *Phys. Rev. B* **78**, 052502 (2008).
- ¹⁷D. Wu, N. Barisic, N. Drichko, S. Kaiser, A. Faridian, M.

- Dressel, S. Jiang, Z. Ren, L. J. Li, G. H. Cao, Z. A. Xu, H. S. Jeevan, and P. Gegenwart, *Phys. Rev. B* **79**, 155103 (2009).
- ¹⁸C. F. Miclea, M. Nicklas, H. S. Jeevan, D. Kasinathan, Z. Hossain, H. Rosner, P. Gegenwart, C. Geibel, and F. Steglich, *Phys. Rev. B* **79**, 212509 (2009).
- ¹⁹Z. Ren, Q. Tao, S. Jiang, C. Feng, C. Wang, J. Dai, G. Cao, and Z. Xu, *Phys. Rev. Lett.* **102**, 137002 (2009).
- ²⁰Q. Zheng, Y. He, T. Wu, G. Wu, H. Chen, J. Ying, R. Liu, X. Wang, Y. Xie, Y. Yan, Q. Li, and X. Chen, [arXiv:0907.5547](https://arxiv.org/abs/0907.5547) (unpublished).
- ²¹S. J. Moon, J. H. Shin, D. Parker, W. S. Choi, I. I. Mazin, Y. S. Lee, J. Y. Kim, N. H. Sung, B. K. Cho, S. H. Kim, J. S. Kim, K. H. Kim, and T. W. Noh, *Phys. Rev. B* **81**, 205114 (2010).
- ²²E. Dengler, J. Deisenhofer, H.-A. Krug von Nidda, Seunghyun Kim, J. S. Kim, Kee Hoon Kim, F. Casper, C. Felser, and A. Loidl, *Phys. Rev. B* **81**, 024406 (2010).
- ²³H. S. Jeevan and P. Gegenwart, *J. Phys.: Conf. Ser.* **200**, 012060 (2010).
- ²⁴Anupam, P. L. Paulose, H. S. Jeevan, C. Geibel, and Z. Hossain, *J. Phys.: Condens. Matter* **21**, 265701 (2009).
- ²⁵V. A. Gasparov, H. S. Jeevan, and P. Gegenwart, *JETP Lett.* **89**, 294 (2009).
- ²⁶S. E. Barnes, *Adv. Phys.* **30**, 801 (1981).
- ²⁷K. W. Blazey, K. A. Müller, J. G. Bednorz, W. Berlinger, G. Amoretti, E. Buluggiu, A. Vera, and F. C. Matocotta, *Phys. Rev. B* **36**, 7241 (1987).
- ²⁸G. F. Goya, R. C. Mercader, L. B. Steren, R. D. Sanchez, M. T. Causa, and M. Tovar, *J. Phys.: Condens. Matter* **8**, 4529 (1996).
- ²⁹A. Abragam and B. Bleaney, *Electron Paramagnetic Resonance of Transition Ions* (Clarendon Press, Oxford, 1970).
- ³⁰J. Deisenhofer, H.-A. Krug von Nidda, A. Loidl, K. Ahn, R. K. Kremer, and A. Simon, *Phys. Rev. B* **69**, 104407 (2004).
- ³¹D. V. Zakharov, J. Deisenhofer, H.-A. Krug von Nidda, A. Loidl, T. Nakajima, and Y. Ueda, *Phys. Rev. B* **78**, 235105 (2008).
- ³²R. H. Taylor, *Adv. Phys.* **24**, 681 (1975).
- ³³B. Elschner and A. Loidl, in *Handbook on the Physics and Chemistry of Rare Earth*, edited by K. A. Gschneidner, Jr. and L. Eyring (Elsevier Science B. V., Amsterdam, 1997), Vol. 24, p. 221.
- ³⁴M. Yashima, H. Nishimura, H. Mukuda, Y. Kitaoka, K. Miyazawa, P. M. Shirage, K. Kiho, H. Kito, H. Eisaki, and A. Iyo, *J. Phys. Soc. Jpn.* **78**, 103702 (2009).
- ³⁵J. J. Ying, T. Wu, Q. J. Zheng, Y. He, G. Wu, Q. J. Li, Y. J. Yan, Y. L. Xie, R. H. Liu, X. F. Wang, and X. H. Chen, *Phys. Rev. B* **81**, 052503 (2010).
- ³⁶H. Fukazawa, Y. Yamada, K. Kondo, T. Saito, Y. Kohori, K. Kuga, Y. Matsumoto, S. Nabaksuji, J. Kito, P. M. Shirage, K. Kihou, N. Takeshita, C.-H.- Lee, A. Iyo, and H. Eisaki, *J. Phys. Soc. Jpn.* **78**, 083712 (2009).
- ³⁷D. Parker, O. V. Dolgov, M. M. Korshunov, A. A. Golubov, and I. I. Mazin, *Phys. Rev. B* **78**, 134524 (2008).
- ³⁸Y. Kobayashi, A. Kawabata, S. C. Lee, T. Moyoshi, and M. Sato, *J. Phys. Soc. Jpn.* **78**, 073704 (2009).
- ³⁹S. W. Zhang, L. Ma, Y. D. Hou, J. Zhang, T.-L. Xia, G. F. Chen, J. P. Hu, G. M. Luke, and W. Yu, *Phys. Rev. B* **81**, 012503 (2010).